**SOLUTION MINING RESEARCH INSTITUTE**
www.solutionmining.org

105 Apple Valley Circle
Clarks Summit, PA 18411, USA

Telephone: +1 570-585-8092

Technical Conference Paper

# A Cavern Abandonment Test at Gellenoncourt, Lorraine
# − An Update −

Benoît Brouard, Brouard Consulting SAS, France
Pierre Bérest, LMS, Ecole Polytechnique, France
Emmanuel Hertz and Cédric Lheur, CSME, France

SMRI Fall 2017 Technical Conference
25 - 26 September 2017
Münster, Germany

Solution Mining Research Institute Fall 2017 Technical Conference
Münster, Germany, 25 - 26 September 2017

# A Cavern Abandonment Test at Gellenoncourt, Lorraine

# − An Update −

Benoît Brouard
Brouard Consulting SAS, 101 rue du Temple, 75003 Paris, France

Pierre Bérest
LMS, Ecole Polytechnique, Route de Saclay, 91128 Palaiseau, France

Emmanuel Hertz and Cédric Lheur
Compagnie des Salins du Midi et des Salines de l'Est, Varangéville, France

## Abstract

CSME operates a brine field at shallow depth at Gellenoncourt, Lorraine, France. An abandonment test, based on the trial-and-error method, began at June 10, 2010. This test consists of monitoring wellhead pressure evolution after a cavern is shut-in. Cavern brine temperature is measured to check that thermal equilibrium between cavern brine temperature and rock mass temperature at cavern depth was reached, as proved by brine temperature measurement. At the beginning of the test, cavern pressure is changed from time to time. When pressure consistently increases (respectively, decreases) it can be inferred that cavern pressure is below (respectively, above) the equilibrium pressure such that cavern creep closure exactly equals brine seepage to the salt formation. The first results of this test were presented during the 2013 SMRI Meeting in Avignon, France. The present paper is an update. It is proved that height years after the test began, pressure evolution remains consistent with what was predicted. Cavern closure rate and salt mass permeability can be back-calculated from the test results.

**Key words:** Cavern Plugging and Abandonment, Cavern Testing

## 1. The abandonment issue

In the past decade, there has been concern about the thermohydromechanical behavior of salt caverns after they have been sealed and abandoned. The SMRI has supported several studies and in situ tests relative to this issue (Ratigan, 2003).

After a cavern is closed and abandoned, cavern brine pressure builds up (Wallner & Paar, 1997). The final value of cavern brine pressure is of utmost importance from the environmental protection point of view. Several authors fear that in many cases brine pressure will after some time reach a figure larger than the geostatic pressure (Wolters et al., 2017), possibly leading to hydrofracturing; brine will flow upward through fractures, to shallow water-bearing strata, leading to water pollution, cavern collapse and subsidence.

As described in many papers (Bérest et al., 1997, 2001), there are several physical mechanisms govern pressure build up:

- Cavern creep closure
- Brine thermal expansion
- Brine micro-permeation through rock salt
- Brine leaks through the wellbore

When brine thermal expansion and wellbore leaks can be neglected, cavern pressure slowly reaches an equilibrium pressure which is larger than the halmostatic pressure at cavern depth (i.e., the pressure in a brine-filled cavern opened at ground level) but smaller than the geostatic pressure at cavern depth. This equilibrium pressure is such that cavern convergence rate is balanced exactly by the small brine flow permeating to the rock mass (Bérest el al., 2001). It is clear that the cavern closure rate at equilibrium pressure will be exceedingly slow and that this equilibrium pressure will be reached after a very long period of time (several dozens of centuries). In most cases, ground subsidence will be exceedingly slow.

The results of two in-situ tests, on EZ53 and SPR2 caverns (Figure 2), supported by SMRI clearly support this approach (Bérest et al., 2013). The results of another test supported by the SMRI performed on Staβfurt shallow caverns (Banach and Klafki, 2009) is consistent with the former scenario.

In the following it is proved that a similar test performed at Gellenoncourt, France, during a 6-year long period clearly confirms these results

## 2. The Gellenoncourt caverns

CSME has operated a brine field in Eastern France since 1965. This field includes the Gellenoncourt brine field, described in Buffet (1998). It is located at the eastern (and shallowest) edge of the Keuper bedded-salt formation of Lorraine-Champagne, in which the salt thickness is 150 m (500 ft). Five horizontal sets of salt layers ("faisceaux", or bundles) have been described by geologists. The salt content of this field is highest in the first (shallowest) and third faisceaux. The overburden layers include argillite, dolomite, sandstone and limestone.

During the first half of the 20th Century, single wells were brined out. After 1965, the hydro-fracturing technique was used. For this brine field, cased and cemented wells are drilled to a depth of 280-300 m (920-980 ft) — i.e., at the base of the third faisceau. The horizontal distance between two neighboring wells typically is 120 to 150 m (400 to 500 ft). Through hydro-fracturing, a link is created between two such caverns at the base of the third pencil. Water then is injected in one well and brine is withdrawn from the other well. After some time, the injection and withdrawal wells are switched. The caverns grow, and their roofs actually reach the first pencil. Brining stops when the cavern roof is 10 m (32 ft) below the salt roof. This 10-m-thick salt slab is left to protect the overlying strata, which are prone to weathering when in contact with brine (Buffet, 1998).

In 2007, CSME decided to perform tests to gain a better knowledge of cavern long-term mechanical behavior ("ACSSL" Project). The SG13-SG14 cavern was selected for performing in-situ tests, as this cavern is representative of the field and had been kept idle for a long period of time.

The SG13 and SG14 7"-wells were drilled in May 1975, and operated as brine-production caverns from July 1976 to June 1977 (SG13), and from October 1978 to July 1980 (SG14). After some time, the two caverns coalesced, and SG13-SG14 now is composed of two parts connected by a large link; hydraulically, they can be considered as a single cavern. A 3D view is provided in Figure 1. From latest sonar measurements (2000), it was inferred that the volumes of SG13 and SG14 are 107,000 $m^3$ (0.67 MMbbls) and 34,000 $m^3$ (0.40 MMbbls), respectively. However, sonar measurements are likely to underestimate the overall cavern volume, as they cannot "see" the insoluble-filled link between the two caverns. Cavern volume at the end of the mining operations also can be inferred from "mass balance"; i.e., from the cumulated amounts of injected water and withdrawn brine during mining operations. "Mass balance" suggests that the actual cavern volume might be as large as $V \approx 240,000\ \mathrm{m}^3$ (1.5 MMbbls).


**Figure 1 - 3D view of the SG13-SG14 cavern (From November 2000 sonar survey; the cavern is viewed from East to West with a 10° downward dip angle.**

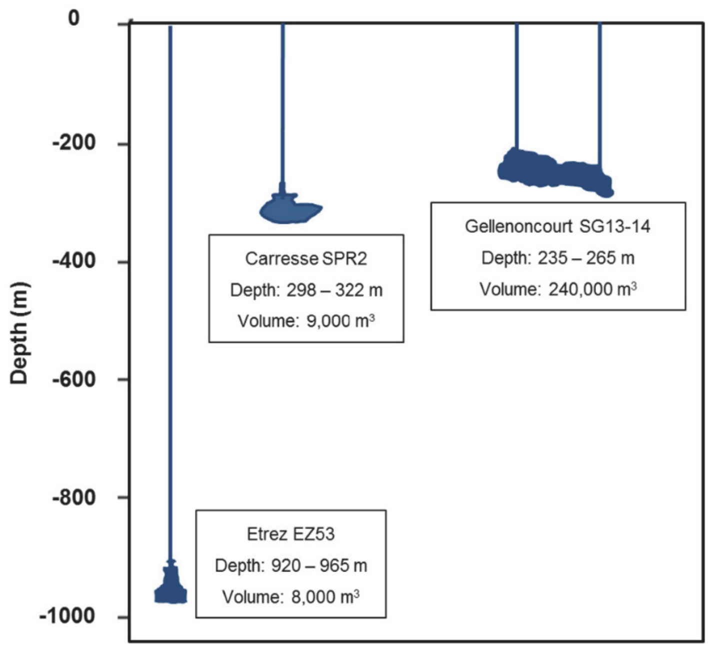


**Figure 2 - Shape and depth of the EZ53, SPR2 and SG13-14 caverns.**

## 3. SG13-SG14 - Cavern temperature evolution

Brine thermal contraction (or expansion) results from the gap between the temperature of the cavern brine and the geothermal temperature of the rock. When cavern brine is warmer than the rock mass, heat is transferred from the cavern to the rock mass through conduction, resulting in brine cooling. Brine cooling generates brine cavern contraction, making brine outflow rate or wellhead pressure rate slower. The brine cooling process is slow —even slower in a larger cavern. In a cavern with volume as $V \approx 240,000 \text{ m}^3$ (1.5 MMbbls), the temperature gap between rock mass temperature and brine cavern temperature which existed at the end of the leaching period is divided by a factor of 4 after 10 years (Karimi et al., 2007). For the SG13-SG14 cavern, soft water injected during the leaching process was slightly warmer (20°C or 68°F) than the geothermal temperature of the rock, which typically is 17.6°C (63,7°F) at cavern depth. The initial gap was small. Moreover, the cavern had been kept idle for nearly 30 years by the time the abandonment test began. It was believed that temperature decrease rate was exceedingly slow at that time.

By December 2008, a temperature sensor was lowered into the SG13 well to assess changes in brine cavern temperature. The cavern temperature was measured at a 247-m depth (810 ft) and remained perfectly constant during the period December 2008 – November 2010. In June 2010, cavern temperature was measured again using the same sensor; sensor depth was 244 m or 800 ft (the small difference in sensor depth is not significant, as natural convection is active in the cavern and vertical temperature gradient in the cavern brine is small) and brine temperature was exactly the same as in December 2008. Sensor resolution was tested as follows: cavern pressure was increased by $\Delta P_c = 1 \text{ MPa}$ (145 psi) by injecting brine during one day. During such a short period of time, brine evolutions are almost perfectly adiabatic and a temperature $\Delta T_c = \alpha_b T_c \Delta P_c / \rho_b C_b$ increase could be expected (Gatelier et al., 2008), where $T_c = 290 \text{ K}$ is the absolute brine temperature, $\alpha_b = 4.4 \times 10^{-4}/°\text{C}$ ($2.4 \times 10^{-4}/°\text{F}$) is brine thermal-expansion coefficient, $\rho_b C_b = 4.8 \times 10^6 \text{ J/m}^3\text{-°C}$ is the volumetric heat capacity of brine, or $\Delta T_c(°\text{C}) = 0.03 \Delta P_c$ (MPa), or $\Delta T_c(°\text{F}) = 0.37 \Delta P_c$ (kpsi). In fact, sensor temperature indication "jumped" by 0.02°C when pressure increase proving that the sensor was sensitive and that its resolution was 0.02°C. For the 18-month temperature measurement period, it can be inferred that temperature rate is slower than — possibly much slower, as the initial temperature gap was small in 1988, almost 30 years before the test.

## 4. SG13-SG14 Abandonment test

In the framework of ACSSL project, a trial-and-error test began on SG13-SG14 in June 2010 and is currently on-going. Downhole and wellhead pressures and temperatures are measured continuously every 5 minutes for more than 7 years, providing a huge amount of data.

A ‘‘trial and error’’ process (Figure 3) consists in approaching the expected steady-state pressure, which was roughly estimated before the test. Different pressure levels are tested successively. When the cavern-pressure rate consistently remains negative for a sufficiently long period of time, it is re-adjusted to a slightly smaller value, in hopes of triggering a change in sign for the cavern-pressure rate. Alternatively, when the cavern-pressure rate consistently remains positive for a sufficiently long period of time, it is re-adjusted to a slightly higher value. Re-adjustments are made via small withdrawals or injections of brine in the cavern.

It was not possible to install a permanent "wellbore-leak detection system" (Bérest et al., 2001) as there is no string in this two-well cavern. However, wellbore leaks were deemed to be small as a successful MIT was performed in July 2010 on both wells before the trial-and-error test. In addition, it was known that, before the test, from 2000 to 2008, wellhead pressure had increased by 0.08 MPa, a figure which is not consistent with high leak rates in a cavern in which thermal expansion is exceedingly small and the cavern closure rate is slow.

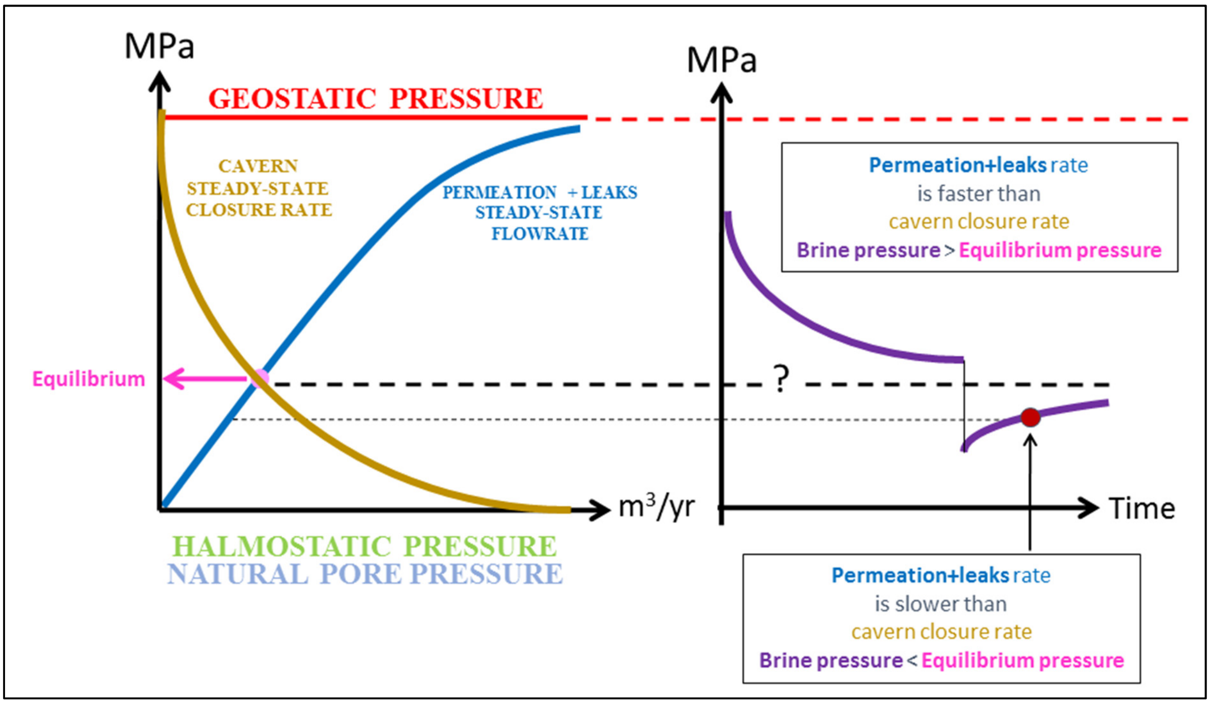


**Figure 3 - Trial and error test when thermal equilibrium is reached.**

Temperature was measured from 2011 to 2017 using the same sensor as in 2010 (see Section 3). An apparent decrease by 0.06°C can be observed during this period (Figure 4). This value is relatively high, as it was assumed that thermal equilibrium was reached. However, it is suspected that the sensor accuracy has slightly deteriorated after a couple of years.

Pressure evolution (Figure 5) clearly proves that equilibrium pressure is not reached yet after seven years. Its value is likely to be $P_{eq} = 34 - 35$ bars (493-508 psi); i.e., significantly smaller than geostatic pressure which, at a $H = 235$ m depth (770 ft), is $P_\infty = 52 - 56$ bars (754-812 psi). The hydrofracturing risk can be disregarded. The cavern-pressure rate becomes exceedingly small, in the order of 0.1 bar/yr or 1.5 psi/yr (Figure 6).

Creep rate and rock permeability can be assessed tentatively as follow. Before the test, a shut-in pressure test and a brine outflow test were performed to assess creep closure rate when cavern pressure is halmostatic, $P = P_h$ (Brouard et al., 2009). The shut-in pressure test proved that cavern closure rate was $\dot{\varepsilon}_{cr} = \dot{V}/V \approx -0.93 \times 10^{-5}$ /yr and $\dot{\varepsilon}_{cr} V = -\beta V \dot{P} \approx -6.1$ liters/day $= -2.2$ m$^3$/yr. (Cavern compressibility, or $\beta V$, had been measured before the test; it is $\beta V = 129.5$ m$^3$/MPa.) The brine outflow test was more difficult to interpret (Figure 7). In fact, after a rapid drop in atmospheric pressure, brine flow sometimes may be very fast during a couple of minutes (Figure 8). This phenomenon is described in Appendix.

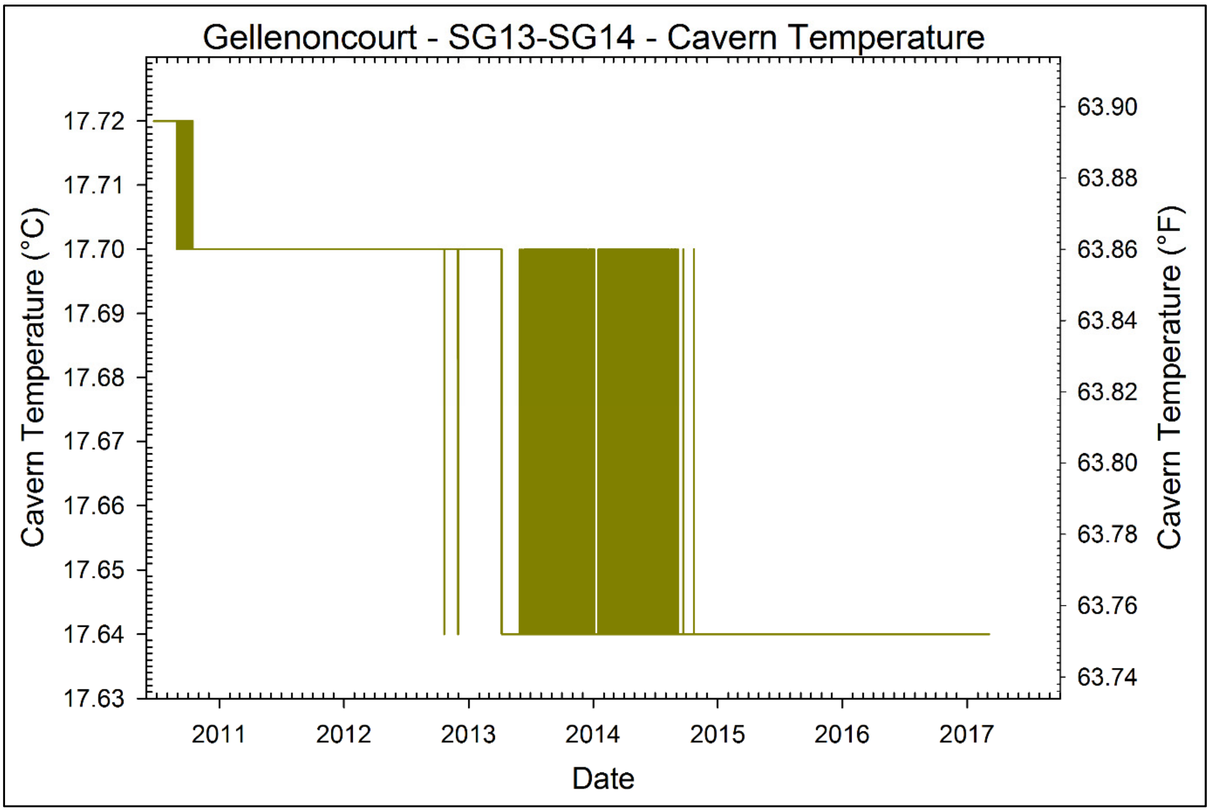


**Figure 4 - Evolution of cavern temperature from 2010 to 2017.**

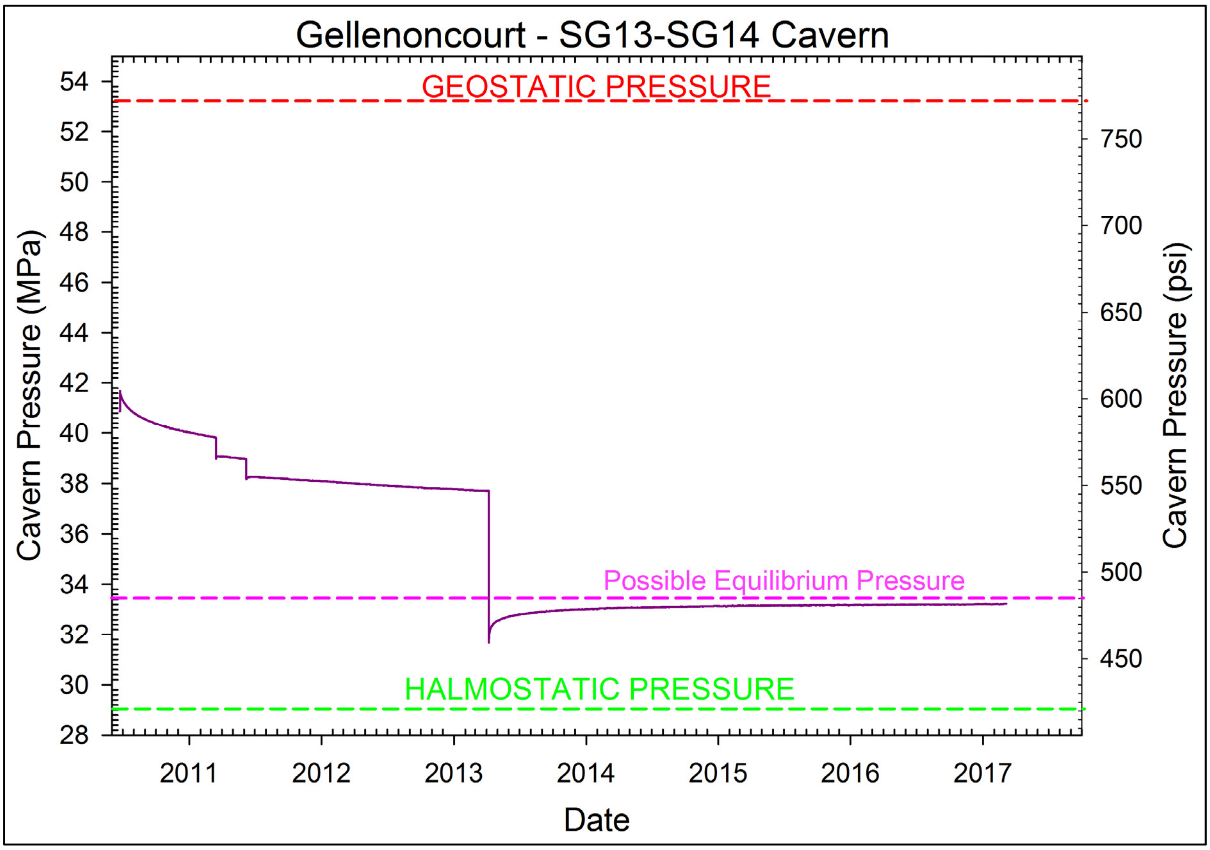


**Figure 5 – Evolution of cavern pressure from 2010 to 2017.**

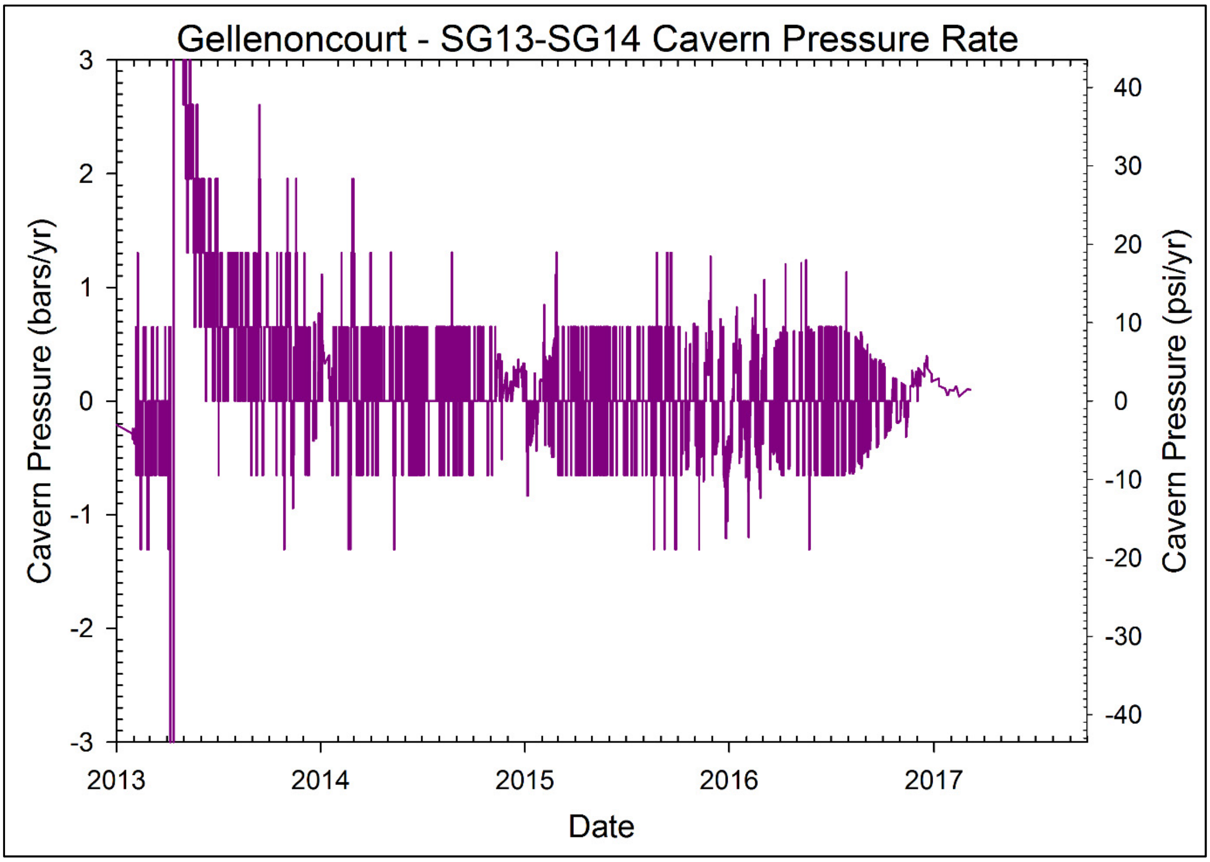


**Figure 6 – Evolution of cavern pressure rate from 2010 to 2017.**

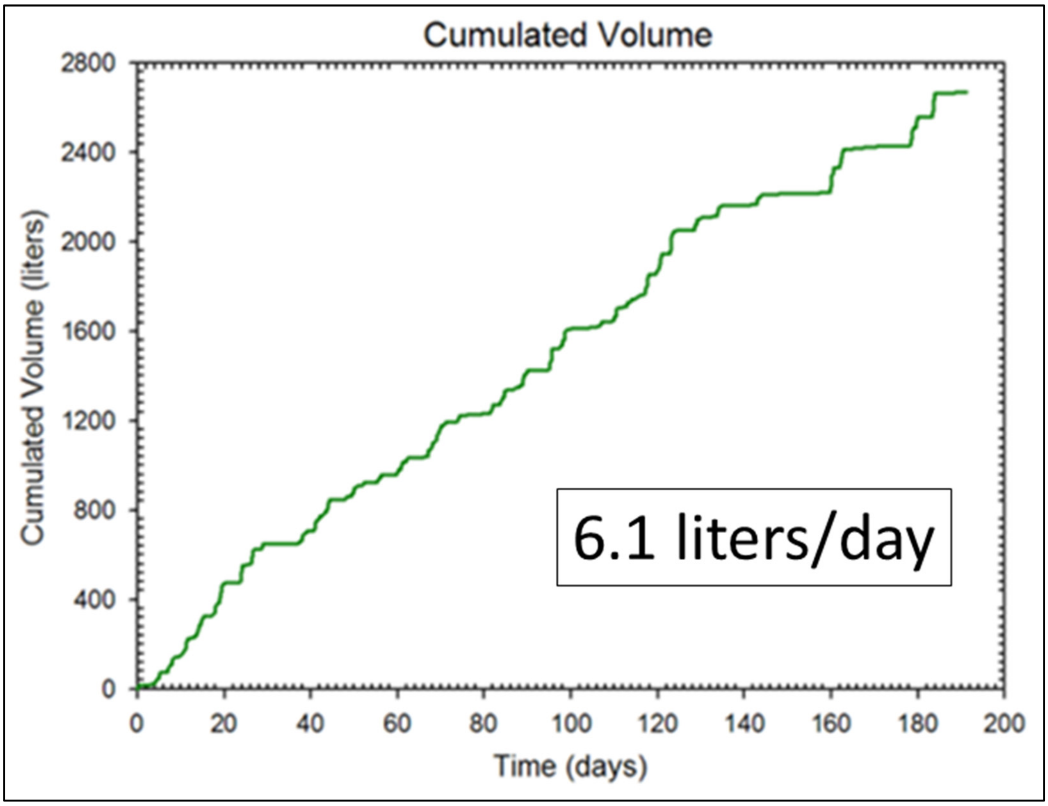


**Figure 7 - Cumulated outflow volume during a 200-day period in 2008.**

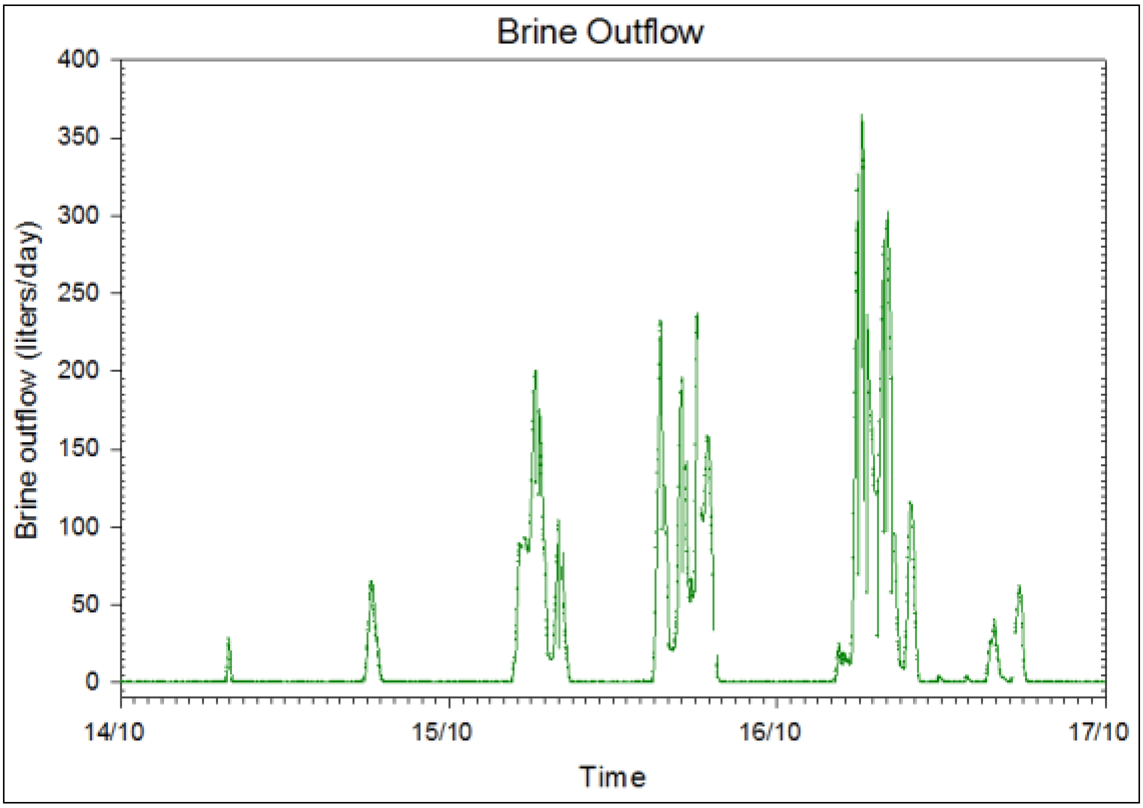


**Figure 8 - Fluctuations of the brine outflow rate during a 3-day long period.**

### Long-term equilibrium pressure

When it is assumed that salt behavior can be described by a power (Norton-Hoff) law and that the exponent of the power law is $n=3$, cavern creep closure when equilibrium pressure is reached is $Vd\varepsilon_{cr}/dt\ \left(P=P_{eq}\right)=Vd\varepsilon_{cr}/dt\ \left(P=P_h\right)\left[\left(P_\infty-P_{eq}\right)/\left(P_\infty-P_h\right)\right]^n$ (see Figure 9). However recent researches supported by the SMRI (citer le rapport) strongly suggest that, in the low deviatoric stress range – the range of interest in the case of the Gellenoncourt cavern – the exponent of the power law might be $n=1$, leading to much faster creep closure rate (see Figure 9).

In principle, when the exponent of the power law and the actual equilibrium pressure are known, rock mass overall permeability (in $m^3$/MPa or bbls/psi) can be assessed (see Figure 10, the overall permeability is proportional to the slope of the straight line, when closure rate is in $m^3$) and numerical computations, taking into account the actual cavern shape, allow computing the average permeability (in $m^2$). We did not try to make these computations.

It was said that the closure rate is $Vd\varepsilon_{cr}(P=P_h)/dt=6.1\ \text{liters/day}$ when cavern pressure is halmostatic ($P=P_h$). It is assumed that cavern average depth is 250 m (820 ft), typically, from which it can be inferred that halmostatic pressure is $P_h=30\ \text{bars}$ (435 psi). It is assumed that equilibrium pressure and geostatic pressure are $P_{eq}=33.5\ \text{bars}$ (486 psi) and $P_\infty=53\ \text{bars}$ (769 psi), respectively (these figures are tentative), and $\left(P_\infty-P_{eq}\right)/\left(P_\infty-P_h\right)=0.85$. The estimated brine flow which enters the rock mass when equilibrium pressure is reached depends on the selected exponent of the power law. When $n=1$, $Vd\varepsilon_{cr}\left(P=P_{eq}\right)/dt=5.2$ liters/day = 1.9 $m^3$/yr (12 bbls/yr). When $n=3$, this figure is smaller still: $Vd\varepsilon_{cr}\left(P=P_{eq}\right)/dt=3.7$ liters/day = 1.4 $m^3$/yr (8.6 bbls/yr).

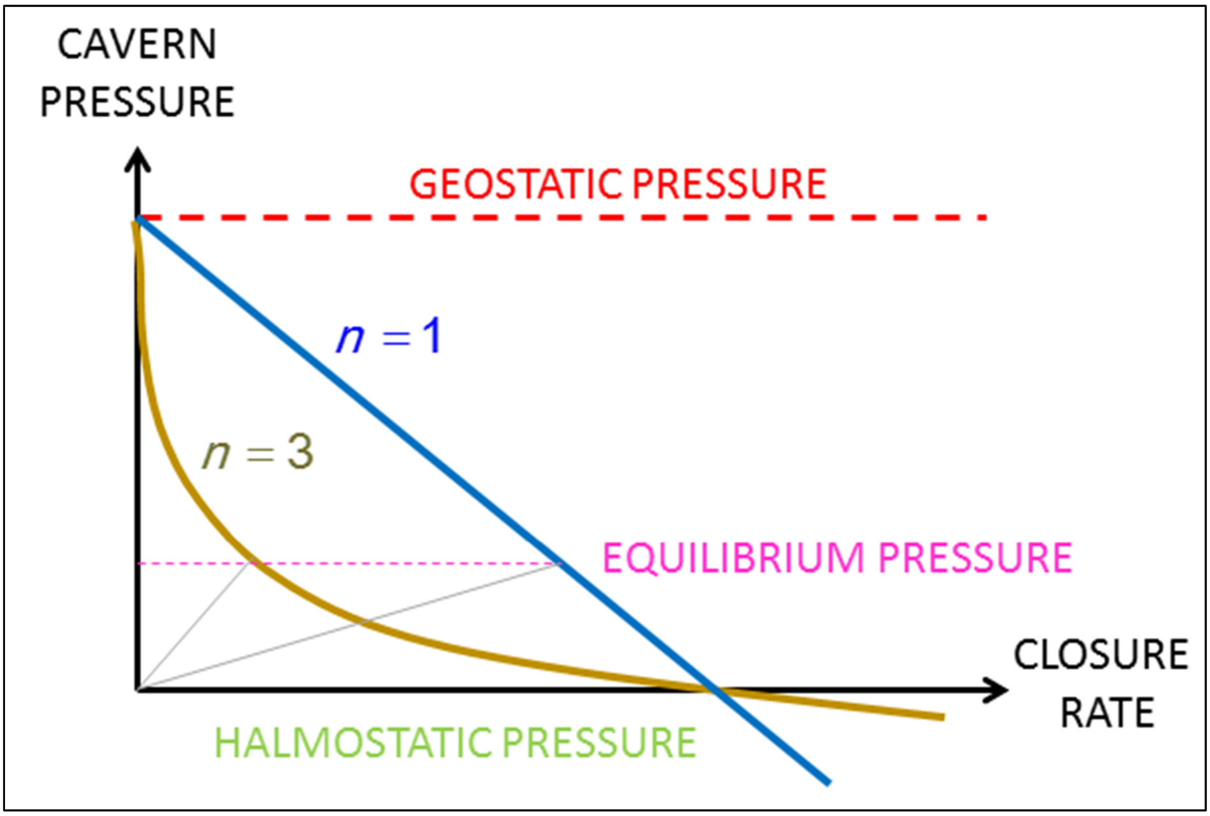


**Figure 9 – Equilibrium pressure depends on the exponent of the creep power law.**

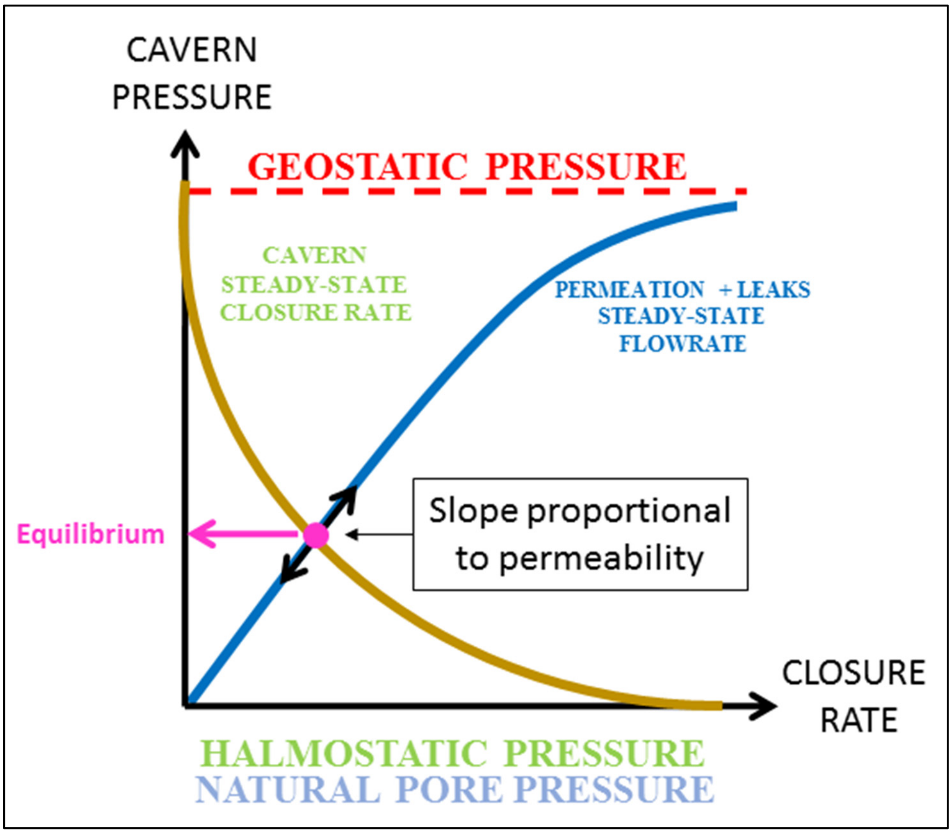


**Figure 10 - The overall permeability is proportional to the slope of the straight line.**

## Acknowledgements

The authors are indebted to the staff of the Gellenoncourt CSME brine field, whose help in performing the tests was invaluable.

## References

Banach A., Klafki M. (2009). *Staßfurt Shallow Cavern Abandonment Field Tests*. SMRI Research Report RR 2009-01.

Bérest P., Brouard B., Durup G. (1997) *Behavior of sealed solution-mined caverns*. Proceedings of Fourth Conference on Mechanical Behaviour of Salt. Clausthal-Zellerfeld, Germany: Trans Tech Pub., p. 511–24.

Bérest P., Brouard B., Hertz E., Lheur C., Hévin G., de Laguérie P., Hardy J.M. (2013). *Cavern abandonment: Three in situ tests*. Proc. SMRI Meeting, Avignon, France, p. 23-36.

Bérest P., Bergues J., Brouard B., Durup JG., Guerber B. (2001) *A salt-cavern abandonment test*. International Journal Rock Mech Min Sci; 38:343-55.

Brouard B., Bérest P., Héas JY., Fourmaintraux D., de Laguérie P., You T. (2004) *An in-situ test in advance of abandoning of a salt cavern*. In: Proceedings SMRI Fall Meeting, Berlin, Germany, 45-64.

Brouard B., Hertz E., Lheur C., Bérest P., de Greef V., Béraud JF. (2009) *A Brine Outflow Test in Gellenoncourt Caverns*. In: Proceedings SMRI Spring Meeting, Krakow, Poland, p. 105-120.

Buffet A. (1998) *The collapse of Compagnie des Salins SG4 and SG5 drillings*. In: Proceedings SMRI Fall Meeting, Roma, Italy, p 79-105.

Crotogino F., Kepplinger J. (2006) *Cavern Well Abandonment Techniques Guidelines Manual*. Report 2006-3 for the SMRI.

Gatelier N., You T., Bérest P., Brouard B. (2008) *"Adiabatic" temperature changes in an oil-filled cavern*. In: Proceedings SMRI Fall Meeting, Galveston, TX, p. 81-104.

Karimi-Jafari M., Bérest P., Brouard B. (2007) Thermal Effects in Salt Caverns. In: Proceedings SMRI Spring Meeting, Basel, Switzerland, p. 179-188.

Wolters R., Lux K.H., Düsterloh U. (2017). *Rock Mechanics Investigations regarding the proof of long-term safety of abandoned salt production cavities using hazardous waste as backfill material*. Proc. SMRI Spring Meeting, Albuquerque, New Mexico, p. 51-70

Ratigan J. (2003). *The SMRI Cavern Sealing & Abandonment Research Program Summary*. Proc. SMRI Spring Meeting, Houston, Texas, p. 141-164.

Wallner M., Paar WA. (1997) *Risk of progressive pressure build up in a sealed cavity*. Proceedings of SMRI Fall Meeting, El Paso, 1997. p. 177–88.

## Appendix – Outflow after a rapid drop in atmospheric pressure

### Brine Outflow Test

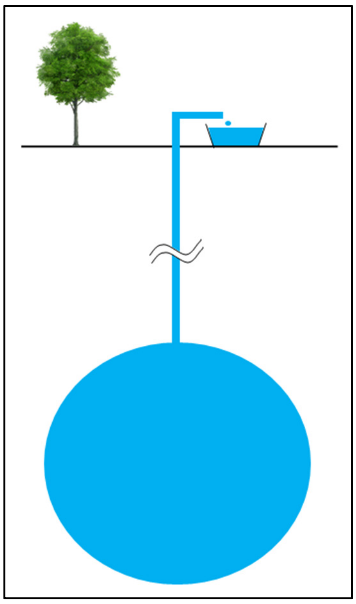

**Figure 11 – Outflow test.**

A brine outflow test is discussed. Both the cavern and the wellbore are filled with saturated brine (Figure 11). The wellhead is opened and a container is set at ground level to collect the expelled brine whose mass is measured.

Cavern slowly shrinks. Cavern creep-closure rate is $\dot{\varepsilon}_{cr} V > 0$ where $V$ is the cavern volume. When the cavern average depth is *H* = 250-m (835 ft) deep, $\dot{\varepsilon}_{cr} = 10^{-5}$/yr is typical; when cavern average depth is *H* = 1000 m (3300 ft), $\dot{\varepsilon}_{cr} = 3 \times 10^{-4}$/yr is typical. The (average) outflow rate is

$$Q = \dot{\varepsilon}_{cr} V > 0 \tag{1}$$

In many cases, brine thermal expansion in the cavern must also be taken into account, as it contributes to the total flowrate; this is not discussed here.

It could be expected that during a short period of time (a couple of weeks) creep closure rate (and brine outflow rate) be perfectly constant. In fact, it is not, as atmospheric pressure experiences small changes (by a couple of hPa) during such a period. Atmospheric pressure changes are transmitted to the cavern both through the brine column and through the rock mass. When atmospheric pressure increases by $p_{atm}$, cavern brine pressure increases by the same amount, cavern brine volume decreases by $\beta_b p_{atm}$ and cavern volume increases by $\beta_c p_{atm}$. However, atmospheric pressure is transmitted through the rock mass also, leading to a cavern volume decrease by $\beta_\infty p_{atm}$. Flowrate fluctuations taking into account atmospheric-pressure variations are

$$Q = V \dot{\varepsilon}_{cr} - V(\beta - \beta_\infty) \dot{p}_{atm} \tag{2}$$

where $\beta = \beta_b + \beta_c$ is the coefficient of compressibility of the cavern. The outflow rate is the sum of two terms: the flow due to creep closure and the flow due to atmospheric pressure changes. For instance, $\beta_b = 2.7 \times 10^{-5}$ /bar, $\beta_c = 2.3 \times 10^{-5}$ /bar and $\beta_\infty = 2.7 \times 10^{-5}$ /bar are typical; an atmospheric pressure decrease by $\dot{p}_{atm} = 10 \text{ hPa/day}$ (0.15 psi/day) in a $V = 300{,}000 \text{ m}^3$ (1.9 MMbbls) cavern generates a 69 liters/day (18 gal/day) outflow. At a 300-m depth $\dot{\varepsilon}_{cr} = 10^{-7}$ /day is typical and the out-flow generated by creep closure is 30 liters/day (8 gal/day). Total outflow rate is Q = 100 liters/day.

**Possible onset of a geyser**

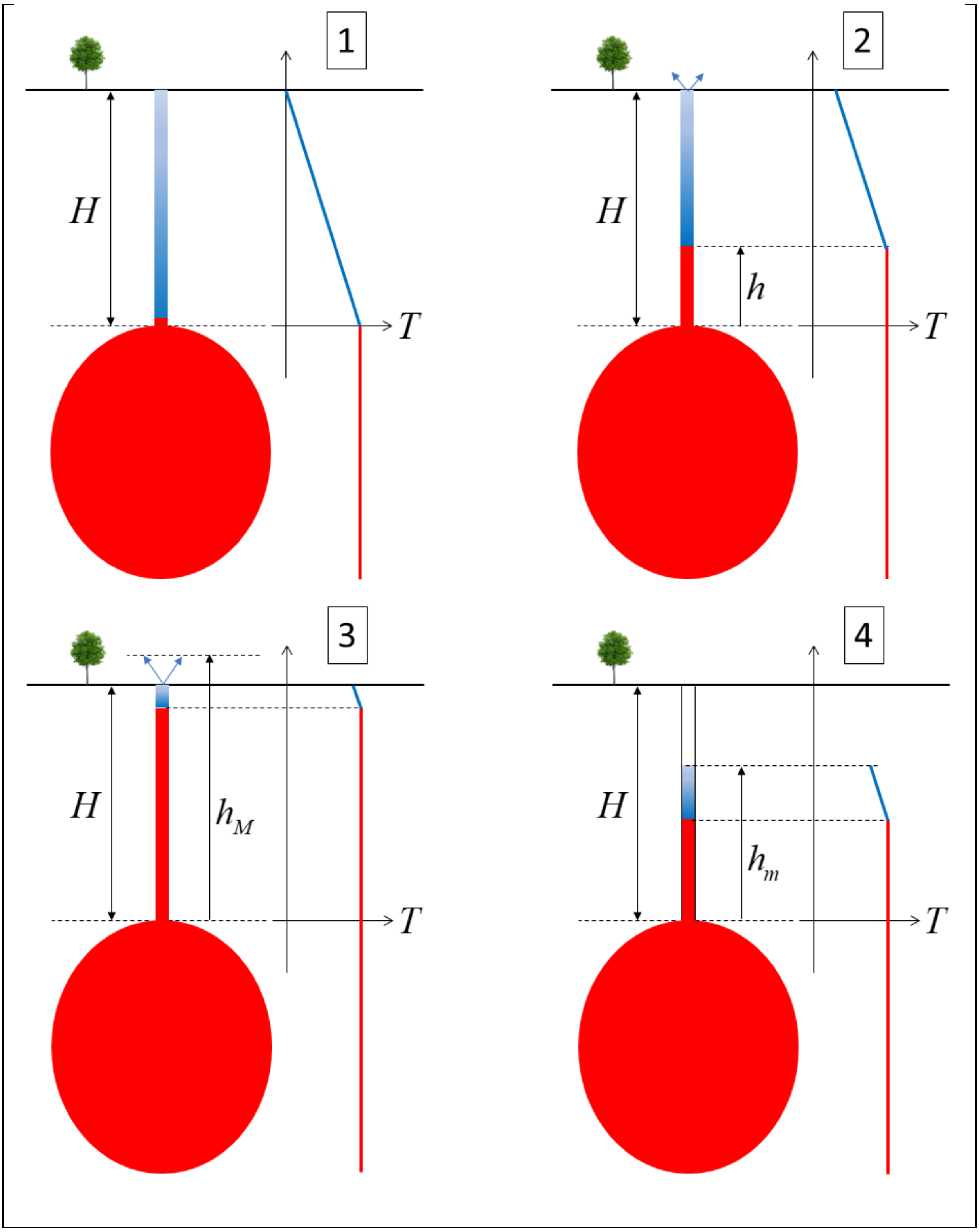


**Figure 12 - Onset of a geyser (2), outflow is maximum (3), end of the outflow (4), final location of the interface.**

In this section, we discuss the stability of the brine outflow and the possible formation of a geyser. The origin of such a geyser is the geothermal gradient. Temperature is an increasing function of depth, $T(z) = T_0 + \Gamma z$, $T_0$ is the temperature at ground level and $\Gamma$ is the geothermal gradient ($\Gamma = 3 \times 10^{-2}/\mathrm{m}$ is typical). In the wellbore, brine is colder at ground level than it is at cavern depth (Figure 12). When brine outflow is slow, at any depth, brine flowing upward in the wellbore is left enough time to reach equilibrium with geothermal temperature. Consider now a fast brine outflow: heat exchange with the rock mass can be neglected and brine keeps its initial temperature when flowing in the borehole. Warm brine enters the wellbore through the casing shoe. At the same time, cold brine is expelled from the wellhead. The average temperature of the brine column increases. Its weight decreases accordingly, and the pressure in the cavern decreases, leading to still faster brine outflow: a geyser is created. Such a geyser can be observed when the cavern is large enough and when wellbore cross sectional area is not too large.

Onset of the geyser is at $t = 0$. Let $h = h(t) > 0$ be the position in the column at time $t > 0$ of the slice of brine which was at depth $H$ at time $t$ = 0, $h$(0) = 0 (Figure 12). The weight of the brine column, which was $\rho_b gSH$ before the geyser starts, decreases by $\rho_b gS\alpha_b \Gamma(2Hh - h^2)/2$; $S$ is the cross-sectional area of the borehole, $g = 10\ \mathrm{m/s^2}$ is gravity acceleration and $\alpha_b = 4.4 \times 10^{-4}/°\mathrm{C}$ is the (adiabatic) thermal expansion coefficient of brine. Newton's first law can be applied to the brine column in the wellbore. Its mass is $\mu = \rho_b HS(1 - \alpha_b \Gamma(2Hh - h^2)/2) \approx \rho_b HS$. Its acceleration is $\ddot{h}$. It is pushed upward by the changes in cavern pressure. These changes include the change in column weight, or $\rho_b gS\alpha_b \Gamma(2Hh - h^2)/2$, and the changes due to cavern compressibility, or $Sh/\beta V$, multiplied by the cross-sectional area. Head losses also must be taken into account; they are assumed here to be proportional to the square of the outflow rate:

$$\rho_b SH\ddot{h} = -\frac{S^2}{\beta V}h + \rho_b g\alpha_b \Gamma\left(\frac{2Hh - h^2}{2}\right)S - F(S)\dot{h}^2 \tag{3}$$

This equation holds when $h < H$; i.e., as long as the wellbore is not completely filled with warm brine. It is convenient to set:

$$\omega^2 = \frac{S}{\rho_b \beta VH}, \quad \gamma^2 = g\alpha_b \Gamma/2 \quad \text{and} \quad f = F(S)/\rho_b SH \tag{4}$$

And the momentum equation can be rewritten:

$$\frac{\ddot{h}}{H} = -\omega^2 \frac{h}{H} + \gamma^2\left(2\frac{h}{H} - \frac{h^2}{H^2}\right) - f\left(\frac{\dot{h}}{H}\right)^2 \quad \text{where } \dot{h} > 0 \text{ and } 0 < h < H \tag{5}$$

This equation can be integrated with respect to time, leading to:

$$\frac{\dot{h}^2}{2H^2} + \frac{\gamma^2}{2f}\left(\frac{h}{H}\right)^2 + \left(\frac{\omega^2 - 2\gamma^2 - \gamma^2/f}{2f}\right)\left(\frac{h}{H} - \frac{1}{2f} + \frac{1}{2f}e^{-2fh/H}\right) = 0 \tag{6}$$

The initial equilibrium position is unstable when the second derivative with respect to $h$ of:

$$\psi(h) = \frac{\gamma^2}{2f}\left(\frac{h}{H}\right)^2 + \left(\frac{\omega^2 - 2\gamma^2 - \gamma^2/f}{2f}\right)\left(\frac{h}{H} - \frac{1}{2f} + \frac{1}{2f}e^{-2fh/H}\right) = 0 \tag{7}$$

is negative, or $\psi(0)=\omega^2-2\gamma^2<0$. This condition is discussed below.

The maximum height reached by the interface, or $h_M$, is obtained when the rate $\dot{h}$ vanishes or:

$$\frac{\gamma^2}{2f}\left(\frac{h_M}{H}\right)^2+\left(\frac{\omega^2-2\gamma^2-\gamma^2/f}{2f}\right)\left(\frac{h_M}{H}-\frac{1}{2f}+\frac{1}{2f}e^{-2fh/H}\right)=0 \tag{8}$$

The height reached by the geyser is $h_M=\dot{h}^2\left[h=H\right]/2g$. (It was assumed that, at the end of the process, the wellbore is not fully filled with warm brine from the cavern, or $h_M<H$. When this assumption does not hold, computations are slightly more complex and are not provided here for simplicity).

After the interface reaches its maximum height, or $h_M$, the brine/air interface drops in the wellbore to $h_m$. Brine mass conservation allows computing $h_m$.

## Discussion

It was proved that a geyser can appear when $\psi(0)=\omega^2-2\gamma^2<0$, or:

$$g\alpha_b\Gamma>\frac{S}{\rho_b\beta VH} \tag{9}$$

The left-hand side of this inequation does not vary much from one site to another, $g\alpha_b\Gamma=10\ \mathrm{m/s^2}\times4{,}4\times10^{-4}/°\mathrm{C}\times3\times10^{-2}\,°\mathrm{C/m}=1.32\times10^{-4}/\mathrm{s}^2$.

A geyser can more likely appear in a large ($V$ is large), deep ($H$ is large) and compressible ($\beta$ is large) cavern when borehole cross-sectional area ($S$) is small enough (possible crystallization must be taken into account, as it makes $S$ smaller). For instance, assume $V=400{,}000\ \mathrm{m}^3$, $\beta=10^{-3}/\mathrm{MPa}$ (it is assumed that the cavern contains gas pockets generated during the leaching process), $\beta V=400\ \mathrm{m^3/MPa}$, $\rho_b=1200\ \mathrm{kg/m^3}$, $H=300\ \mathrm{m}$ and $S=10^{-2}\mathrm{m}^2$ lead to $S/\rho_b\beta VH=0.7\times10^{-4}\mathrm{s}^{-2}$, a figure which is significantly smaller than $g\alpha_b\Gamma=1.32\times10^{-4}/\mathrm{s}^2$, making onset of a geyser highly likely.